Exploring periodicity and dispersion diagrams in muffler design

Vinícius D. Lima[1], Belisário N. Huallpa[2] and José R. F. Arruda[1]

[1]University of Campinas, Rua Mendeleyev, 200, Campinas, SP, Brazil
vinidiaslima@gmail.com, arruda@fem.unicamp.br
[2]Universidade Federal de Lavras, Lavras, Aquenta Sol, MG, Brazil
belisario.nina@deg.ufla.br

Abstract

Periodic waveguides may be analyzed using dispersion diagrams, which plot the wavenumbers as functions of frequency. Imaginary wavenumbers mean propagation is not possible and, therefore, normal modes cannot build up. Muffler design has traditionally explored periodicity, but usually not using dispersion analysis. In this work, we show how to model one-dimensional acoustic waveguides with plane wave assumption using spectral elements (SE), how to obtain dispersion diagrams and, using semi-infinite elements, transmission loss from an SE model. The technological challenge consists in opening band gaps at low frequencies with a limited size muffler, and SE models are handy for low cost parameter optimization. For arbitrary shapes, this work uses scaled SE models or, alternatively, a state-space formulation recently developed by the authors. Additive manufacturing is an enabling technology for the implementation of the designed mufflers. In this work, we show experimental results for simple periodic mufflers built using 3D printing. The proposed simulation methodology is simple and can be used for quick design of 3D-printed polymer mufflers.

1 Introduction

Acoustic mufflers are usually characterized by their insertion loss (IL) or transmission loss (TL) [1]. The latter is a more absolute characterization, as it does not depend upon the acoustic impedance of the system connected to the muffler. Mufflers can be reactive, active of hybrid depending on the sound attenuation mechanism. Reactive mufflers do not need to dissipate energy and attenuate using acoustic impedance discontinuities and acoustic resonators that cause destructive interference. Active mufflers attenuate propagating sound by energy dissipation. Mufflers may combine these two mechanisms. The design of reactive sound mufflers usually start from a chosen geometry combining Helmholtz resonators, quarter length tubes and expansion chambers and adjusting their parameters to maximize the TL at desired frequency ranges.

In recent years, inspired by the scientific advances in photonics [2], researchers started using wave dispersion diagrams of periodic elastic systems to investigate the existence of frequency stop bands created by destructive interference (Bragg scattering) and local resonance due to resonators. This is exactly the effect desired in reactive mufflers. Therefore, in this work, we investigate the use of dispersion diagrams to design periodic reactive mufflers.

Dispersion diagrams are usually obtained using the Plane Wave Expansion (PWE) method [3]. Otherwise, given a transfer matrix of a periodic cell, the Floquet-Bloch theorem can be used to obtain the wavenumbers as a function of frequency. In this work we derive a spectral acoustic element to model the linear acoustics of ducts using the plane wave assumption. It is straightforward to derive a semi-infinite acoustic duct element. Using finite and semi-infinite spectral elements a model can be easily built to compute the TL and simulate the forced responses.

We first introduce the acoustic spectral elements, show how to assemble these elements, how to reduce the global matrix and transform it into a transfer matrix, and, finally, how to compute the dispersion diagram. Then we show how to assemble a duct system consisting of source, uniform duct, periodic muffler and semi-infinite duct that allows computing the TL. We show that with a small number of periodic cells a high TL is achieved. Finally, experimental results obtained in an impedance tube for a 3D-printed periodic muffler are shown.

2 Analytical Formulation

2.1 Acoustic spectral element

The derivation of the acoustic duct spectral element is analogous to the spectral element for elementary rods [4]. Assuming plane wave propagation, the spectral element for an acoustic waveguide starts from the one-dimensional non-dissipative wave equation [5]

$$\frac{\partial^2 p}{\partial x^2} - \frac{1}{c^2}\frac{\partial^2 p}{\partial t^2} = 0 \tag{1}$$

where p is the acoustic pressure at a position x along the waveguide and c is the speed of sound. In the frequency domain, Eq. 1 becomes an ordinary differential equation

$$\frac{\partial^2 \hat{p}}{\partial x^2} + \frac{\omega^2}{c^2}\hat{p} = 0 \tag{2}$$

Equation 2 has a wave-based solution form given by:

$$\hat{p} = C_1 e^{-ikx} + C_2 e^{-ik(L-x)} \tag{3}$$

where k is the wavenumber. For low sound levels, the acoustic pressure and the particle velocity u are related by the linear Euler's equation [5]

$$\rho\frac{\partial u}{\partial t} = -\frac{\partial p}{\partial x} \tag{4}$$

where ρ is the mass density of the fluid. Replacing the solution given by Eq. 3 into Eq. 4 and rearranging in terms of the volume acceleration $\hat{v} = S\partial u/\partial t$ yields

$$\hat{v} = \frac{S}{\rho c}\left(-C_1 e^{-ikx} + C_2 e^{-ik(L-x)}\right) \tag{5}$$

where S is the cross-sectional area.

Considering a straight acoustic waveguide with length L, constants C_1 and C_2 can be determined for given boundary conditions at $x = 0$ and $x = L$. Finding the solution for these constants yields the following matrix system [4] [6]:

$$\begin{bmatrix}\hat{V}_l \\ \hat{V}_r\end{bmatrix} = \frac{ikS}{\rho(1-e^{-2ikL})}\begin{bmatrix}1+e^{-2ikL} & -2e^{-ikL} \\ -2e^{-ikL} & 1+e^{-2ikL}\end{bmatrix}\begin{bmatrix}\hat{p}_l \\ \hat{p}_r\end{bmatrix} = \begin{bmatrix}D_{ll} & D_{lr} \\ D_{rl} & D_{rr}\end{bmatrix}\begin{bmatrix}\hat{p}_l \\ \hat{p}_r\end{bmatrix} = \mathbf{D}\begin{bmatrix}\hat{p}_l \\ \hat{p}_r\end{bmatrix} \tag{6}$$

where $\mathbf{D}$ is the spectral element matrix for the acoustic waveguide.

2.2 Dispersion diagram

An acoustic tube with periodically varying cross section ca be called a phononic crystal [2]. The band structure of a phononic crystal may be represented by a dispersion diagram, i.e., a plot of the wavenumber versus frequency (or vice-versa). A transfer matrix relates the acoustic pressure and the volume acceleration at the left and right ends of a periodic cell as

$$\begin{bmatrix}\hat{p}_r \\ -\hat{V}_r\end{bmatrix} = \mathbf{T}\begin{bmatrix}\hat{p}_l \\ \hat{V}_l\end{bmatrix} = \begin{bmatrix}-D_{ll}D_{lr}^{-1} & -D_{lr}^{-1} \\ D_{rl} - D_{ll}D_{rr}D_{lr}^{-1} & -D_{rr}D_{lr}^{-1}\end{bmatrix}\begin{bmatrix}\hat{p}_l \\ \hat{V}_l\end{bmatrix} \tag{7}$$

The transfer matrix of a periodic system with n cells can be obtained from the matrices of each cell $\mathbf{T_1}, \mathbf{T_2}, ..., \mathbf{T_{n-1}}, \mathbf{T_n}$ as

$$\mathbf{T} = \mathbf{T_n}\mathbf{T_{n-1}}...\mathbf{T_2}\mathbf{T_1} \tag{8}$$

The Floquet-Bloch theorem states the relation between the state vector at the right and left boundaries of the unit cell as

$$\begin{bmatrix} \hat{p}_r \\ -\hat{V}_r \end{bmatrix} = e^{-ikL} \begin{bmatrix} \hat{p}_l \\ \hat{V}_l \end{bmatrix} \tag{9}$$

Equations 7 and 9 yield the following eigenproblem:

$$\mathbf{T} \begin{bmatrix} \hat{p}_l \\ \hat{V}_l \end{bmatrix} = e^{-ikL} \begin{bmatrix} \hat{p}_l \\ \hat{V}_l \end{bmatrix} = \lambda \begin{bmatrix} \hat{p}_l \\ \hat{V}_l \end{bmatrix} \tag{10}$$

The solution of the eigenproblem in Eq. 10 gives the normalized wavenumber kL for each angular frequency ω using the relation

$$kL = i \ln(\lambda) \tag{11}$$

2.3 Transmission loss

In this section we recall the two-load method for computing the TL with an impedance tube. The loudspeaker is positioned at the left extremity, and measurements are performed with two different terminations at the right end. The sample is positioned at the central position, with two microphones measuring the pressures at each side. With the positions of the microphones and the pressures, the amplitudes of the transmitted and reflected waves can be determined by

$$A = i\sqrt{G_{rr}} \frac{H_{1r}e^{ikx_2} - H_{2r}e^{ikx_1}}{2\sin k(x_1 - x_2)} \tag{12a}$$

$$B = i\sqrt{G_{rr}} \frac{H_{2r}e^{-ikx_1} - H_{1r}e^{-ikx_2}}{2\sin k(x_1 - x_2)} \tag{12b}$$

$$C = i\sqrt{G_{rr}} \frac{H_{3r}e^{ikx_4} - H_{4r}e^{ikx_3}}{2\sin k(x_3 - x_4)} \tag{12c}$$

$$D = i\sqrt{G_{rr}} \frac{H_{4r}e^{-ikx_3} - H_{3r}e^{-ikx_4}}{2\sin k(x_3 - x_4)} \tag{12d}$$

where G_{rr} is the autospectrum of the loudspeaker signal (there is no need to use the actual loudspeaker velocity, the voltage input signal is sufficient) and H_{nr} and x_n are the frequency response functions (FRF) for input r and output pressure measured with microphones $n = 1,2,3,4$. The pressures and particle velocities at the sample extremities are given by

$$p_0 = A + B \tag{13a}$$

$$u_0 = \frac{(A - B)}{\rho c} \tag{13b}$$

$$p_d = Ce^{-jkd} + De^{-jkd} \tag{13c}$$

$$u_d = \frac{Ce^{-jkd} - De^{-jkd}}{\rho c} \tag{13d}$$

Denoting with subscripts a and b the measurements with two different tube terminations (e.g. open and closed), the transfer matrix of the sample can be determined by

$$\begin{bmatrix} T_{11} & T_{12} \\ T_{21} & T_{22} \end{bmatrix} = \frac{1}{p_{da}v_{db} - p_{db}v_{da}} \begin{bmatrix} p_{0a}v_{db} - p_{0b}v_{da} & p_{0b}p_{da} - p_{0a}p_{db} \\ v_{0a}v_{db} - v_{0b}v_{da} & p_{da}v_{0b} - p_{db}v_{0a} \end{bmatrix} \tag{14}$$

The transmission loss of the sample is obtained by:

$$TL = 20\log_{10} \left| \frac{1}{2} \left(T_{11} + \frac{T_{12}}{\rho c} + \rho c T_{21} + T_{22} \right) \right| \tag{15}$$

In the cases where the sample is symmetric, another two conditions can be set, and only one load is necessary to determine the transfer matrix. These conditions are the reciprocity and symmetry given by

$$T_{11} = T_{22} \tag{16a}$$

$$T_{11}T_{22} - T_{12}T_{21} = 1 \tag{16b}$$

With the conditions of Eqs. 16 the transfer matrix is determined by:

$$\begin{bmatrix} T_{11} & T_{12} \\ T_{21} & T_{22} \end{bmatrix} = \frac{1}{p_0 v_d + p_d v_0} \begin{bmatrix} p_d v_d + p_0 v_0 & p_0^2 - p_d^2 \\ v_0^2 - v_d^2 & p_d v_d + p_0 v_0 \end{bmatrix} \tag{17}$$

where subscripts a and b are no longer necessary.

2.4 Insertion loss

The insertion loss is the difference between the acoustic power transmitted with and without the muffler, denoted by the subscripts 2 and 1, respectively

$$IL = L_{W_1} - L_{W_2} = 10 \log \left(\frac{W_1}{W_2} \right) \tag{18}$$

If the temperature gradient is negligible and the source pressure is constant [1] it becomes simply

$$IL = 20 \log \left| \frac{p_1}{p_2} \right| \tag{19}$$

where p_1 is the pressure at the outlet without the muffler and p_2 with the muffler.

3 Numerical results

Using the spectral element previously derived, the periodic muffler can be modeled by assembling the element matrices by imposing continuity at the element connections. Two connected elements are assembled as

$$\mathbf{D} = \begin{bmatrix} D_{ll}^{(1)} & D_{lr}^{(1)} & 0 \\ D_{rl}^{(1)} & D_{rr}^{(1)} + D_{ll}^{(2)} & D_{lr}^{(2)} \\ 0 & D_{rl}^{(2)} & D_{rr}^{(2)} \end{bmatrix} \tag{20}$$

After assembling all the elements composing the periodic cell, the resulting matrix can be condensed to the nodes at the two ends, resulting in a 2 x 2 matrix

$$\bar{\mathbf{D}} = \begin{bmatrix} D_{11} - D_{21} D_{22}^{-1} D_{12} & -D_{23} D_{22}^{-1} D_{12} \\ -D_{21} D_{22}^{-1} D_{32} & D_{33} - D_{32} D_{22}^{-1} D_{23} \end{bmatrix} \tag{21}$$

which can be transformed into a transfer matrix using Eq. 6 , in terms of $\bar{\mathbf{D}}$

$$\mathbf{T} = \begin{bmatrix} -\bar{D}_{12}^{-1} \bar{D}_{11} & \bar{D}_{12}^{-1} \\ -\bar{D}_{21} + \bar{D}_{22} \bar{D}_{12}^{-1} \bar{D}_{11} & -\bar{D}_{12}^{-1} \bar{D}_{22} \end{bmatrix} \tag{22}$$

From the transfer matrix of the periodic cell the dispersion relation is computed as previously described. It is shown in Fig. 2. Furthermore, using Eq. 15, the TL can be computed, as shown in Fig. 1. To compute the FRFs for a volume acceleration input at one end and pressure outputs at the two ends matrix $\bar{\mathbf{D}}$ is inverted and multiplied by vector $\hat{\mathbf{V}} = [1\ 0]^T$.

4 Experimental results

The two loads used in the impedance tube were a rigid and a nearly anechoic termination, implemented using absorptive foam in the open tube end. Figure 4 shows the experimental setup.

The sample is a periodic muffler built using 3D printing (polyamide and selective laser sintering). Figure 5 shows the sample manufactured for the experiment.

Measurements were made with a commercial impedance tube with four-microphones. The loudspeaker was driven with a Gaussian noise signal approximately white (flat spectrum) in the frequency range from 0 Hz to 5272 Hz. A single roving microphone was used to avoid the phase calibration required in the four-microphone measurement [7].

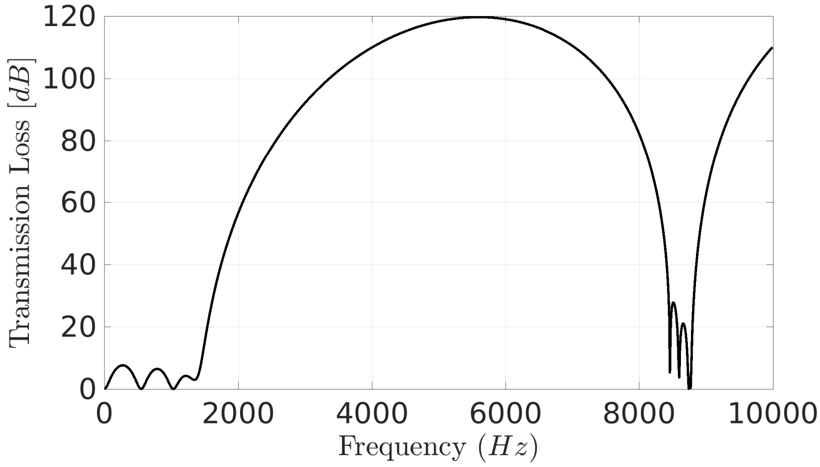

Figure 1: Simulated TL.

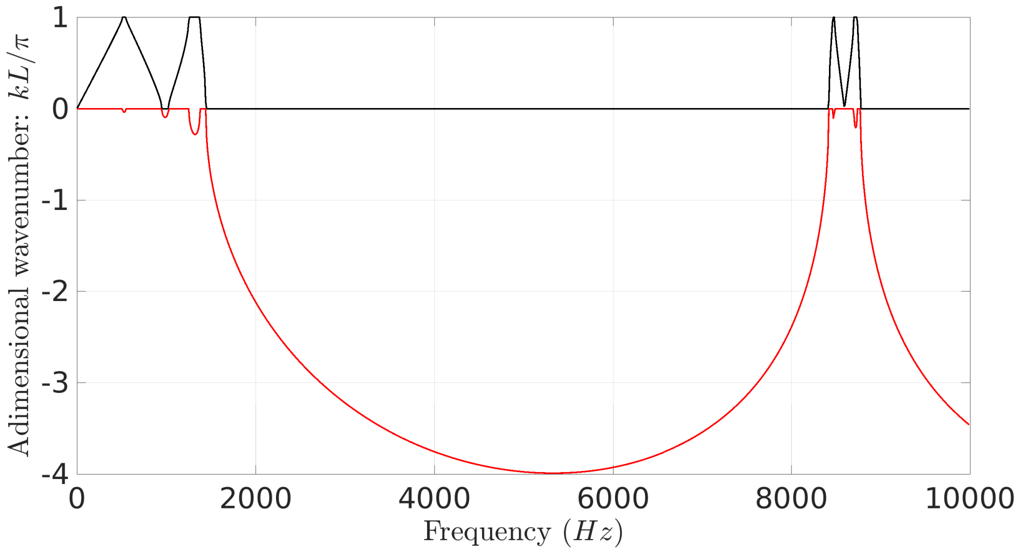

Figure 2: Simulated dispersion diagram.

Figure 6 shows a comparison between simulated and experimental results for the TL. The one-load method, allowed by the symmetric muffler geometry in our case, yielded better results. Experimental background noise did not allow to obtain TL values above approximately 20 dB.

Figure 7 shown a comparison between the predicted and measured IL. The measurements are less noisy, but again background noise did not allow obtaining IL values larger than 20 dB. Measurements inside an anechoic chamber are under way to try to get measurements with lower background noise in the case of the open tube.

5 Conclusions

We have shown how to use dispersion diagrams to predict band gaps in periodic mufflers, which result in large transmission losses. Using acoustic spectral elements it is straightforward to obtain the muffler transfer matrix, from which the dispersion diagram and TL can be computed. For arbitrary shapes, the periodic cell can be computed by discretizing the cell with uniform spectral elements. Otherwise, as shown by the authors [8], a state-space formulation and Riccati-type equation for the acoustic impedance can be used. Optimized mufflers can be constructed using 3D printing. Different optimization strategies are under investigation by the authors. The tools shown in this work set a framework for periodic muffler design optimization using dispersion relations.

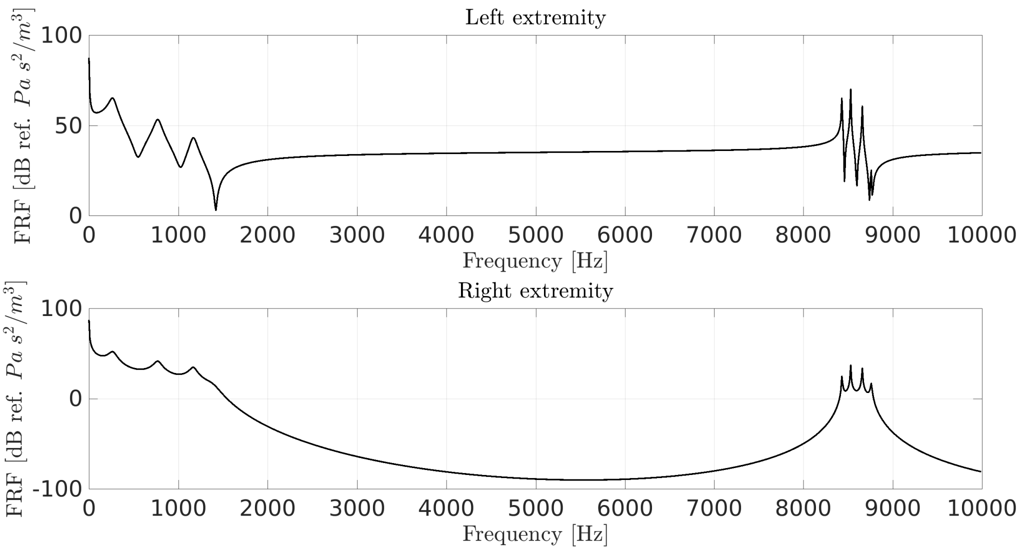

Figure 3: Simulated FRFs.

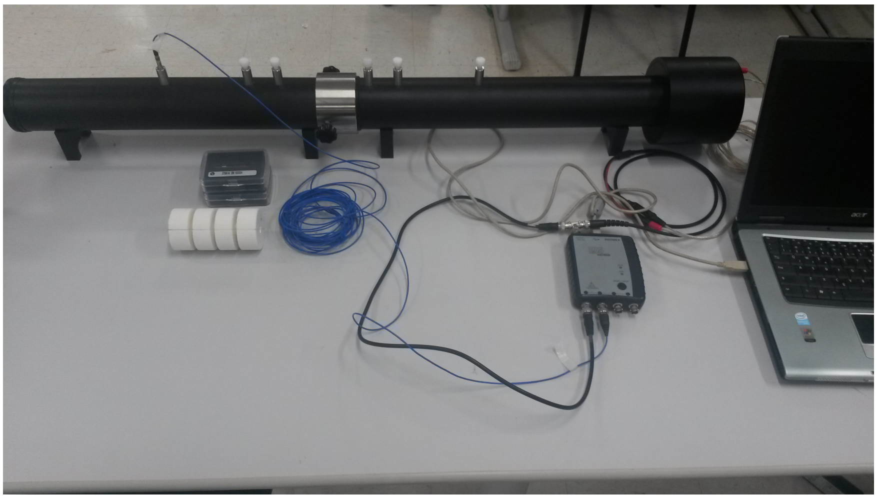

Figure 4: Experimental setup.

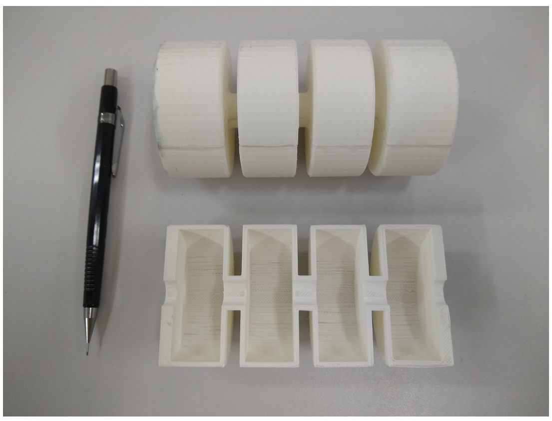

Figure 5: Manufactured muffler.

Acknowledgements

The authors are thankful to Coordenação de Aperfeiçoamento de Pessoal de Nível Superiorl (CAPES Finance Code 001) and the São Paulo Research Foundation (FAPESP 2018/15894-0) for the financial support.

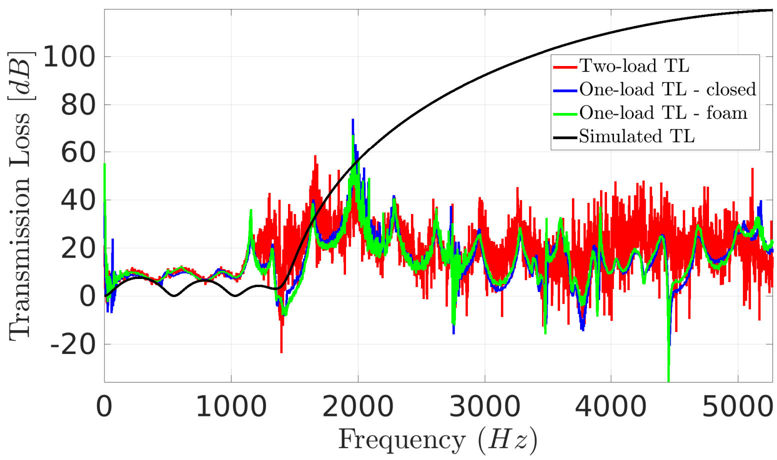

Figure 6: Simulated and experimental transmission loss.

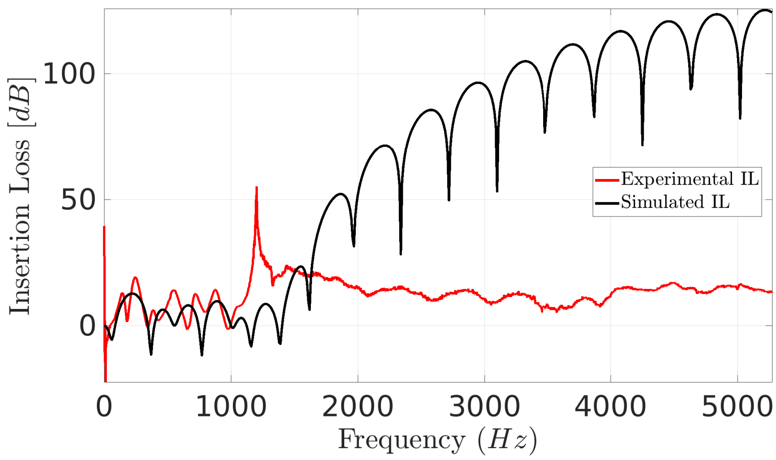

Figure 7: Simulated and experimental insertion loss.

References

[1] M.L. Munjal, *Acoustic of ducts and mufflers with application to exhaust and ventilation system design*, John Wiley and Sons, Canada, 1987.

[2] M.I. Hussein, M.J. Leamy and M. Ruzzene, *Dynamics of phononic materials and structures: Historical origins, recent progress, and future outlook*, Applied Mechanics Reviews, American Society of Mechanical Engineers, 2014, V. 66, n. 4, pp.1-4.

[3] M.M. Sigalas and E.N. Economou, *Elastic and acoustic wave band structure*, Journal of Sound and Vibration, 1992, V. 158, n. 2, pp. 337-382.

[4] J.F. Doyle, *Wave Propagation in Structures: Spectral Analysis Using Fast Discrete Fourier Transforms*, Mechanical Engineering Series, Springer New York, USA, 1997.

[5] L.E. Kinsler, A.R. Frey, A.B. Coppens and J.V. Sanders, *Fundamentals of acoustics*, John Wiley and Sons, USA, 2000.

[6] M. I. N. Rosa, V. D. Lima, J. M. C. Santos and J. R. F. Arruda, *Numerical and Experimental Investigation of Interface Modes in Periodic Acoustic Waveguides*, Proceedings of the International Conference on Structural Engineering Dynamics, Viana do Castelo, Portugal, 24-26 June 2019, 10 pages.

[7] B.H. Song and J.S. Bolton, *A transfer-matrix approach for estimating the characteristic impedance and wave numbers of limp and rigid porous materials*, Journal of the Acoustical Society of America, 2000, V. 107, n. 3, pp.1131-1152,

[8] G.F.C.A. Assis, D. Beli, E.J.P. Miranda Jr., J.F. Camino, J.M.C. dos Santos and J.R.F. Arruda, *Wave Propagation in Structures: Spectral Analysis Using Fast Discrete Fourier Transforms*, International Journal of Mechanical Sciences (submitted), 2019.